Content-dependent on-the-fly visual information fusion for battlefield scenarios

Mathieu Aubailly*[a], Mikhail A. Vorontsov[a,b], Gary Carhart[c], J. Jiang Liu[c], and Richard Espinola[d]
[a]University of Maryland, College Park, MD, USA 20742;
[b]University of Dayton, Dayton, OH, USA 45469;
[c]U.S. Army Research Laboratory, Adelphi, MD, USA 20783;
[d]U.S. Army Communication and Electronics RDE Center, Ft. Belvoir, VA, USA 22060

ABSTRACT

We report on cooperative research program between Army Research Laboratory (ARL), Night Vision and Electronic Sensors Directorate (NVESD), and University of Maryland (UMD). The program aims to develop advanced on-the-fly atmospheric image processing techniques based on local information fusion from a single or multiple monochrome and color live video streams captured by imaging sensors in combat or reconnaissance situations. Local information fusion can be based on various local metrics including local image quality, local image-area motion, spatio-temporal characteristics of image content, etc. Tools developed in this program are used to identify and fuse critical information to enhance target identification and situational understanding in conditions of severe atmospheric turbulence.

Keywords: Imaging through turbulence, lucky-region fusion, high-dynamic range imaging, image enhancement, local image quality.

1. INTRODUCTION

Imaging through a random media such as the Earth's atmosphere commonly causes random local image degradations and distortions. This is especially the case in near-horizontal imaging scenarios which are typical of combat and reconnaissance situations. In order to improve image quality, we previously developed an image processing technique referred to as *lucky-region fusion* (LRF)[1-5]. The LRF technique consists of the following steps: (1) selection of best quality regions (so-called *lucky-regions*) within a set of randomly-distorted images, and (2) fusion of the selected lucky-regions into a fused image which typically features an improved image quality.

A number of improvements had been provided to the original LRF technique including:

- Addition of pre- and post-processing stages for image stabilization (jitter compensation), noise mitigation (image filtering, image destripping), contrast and detail enhancement (pixel-based algorithms, histogram-based algorithms, image sharpening) prior and after performing the LRF algorithm[4],
- Performing the LRF algorithm to a continuous stream of images (as opposed to a finite sequence of images),
- Automation of the fusion kernel calculation for optimal selection of lucky-regions[5] and lucky-region selection using an anisotropic kernel, and
- Mitigation of image fusion artifacts related to moving objects.

More recently, focus was put on imaging of high-dynamic range (HDR) scenes, and multi-spectral/color image fusion. In this paper we report on our progress on these two topics.

2. LUCKY-REGION FUSION TECHNIQUE

2.1 Selection of lucky-regions

Image quality maps (IQMs) are used in the LRF technique in order to select lucky regions within a set of distorted images. An IQM $M(\mathbf{r})$ where vector $\mathbf{r} = \{x, y\}$ denotes the spatial coordinates characterizes locally the quality

*mathieu@umd.edu

Photonic Applications for Aerospace, Transportation, and Harsh Environment III,
edited by Alex A. Kazemi, Nicolas Javahiraly, Allen S. Panahi, Simon Thibault, Bernard C. Kress,
Proc. of SPIE Vol. 8368, 83680J · © 2012 SPIE · CCC code: 0277-786X/12/$18 · doi: 10.1117/12.918681

(sharpness) of an image and is defined as the convolution between a spatially-varying image quality metric $J(\mathbf{r})$ and a Gaussian kernel $G(\mathbf{r},a) = \exp[-|\mathbf{r}|^2/(2a^2)]$:

$$M(\mathbf{r}) = \int J(\mathbf{r}')G(\mathbf{r}-\mathbf{r}',a)d^2\mathbf{r}', \tag{1}$$

where a is a scalar referred to as the fusion kernel size. The IQM quantifies the image quality within a local region of radius a centered on point $\mathbf{r}$. A commonly used image quality metrics $J(\mathbf{r})$ is based on the image gradient and given as $J(\mathbf{r}) = |\nabla I(\mathbf{r})|$, where ∇ denotes the gradient operator and $I(\mathbf{r})$ the image intensity distribution.

2.2 Fusion of lucky-regions

Consider now the fusion of a set $\{I_n(\mathbf{r})\}$ of N randomly-distorted images captured sequentially at times t_n. Lucky-region fusion is performed iteratively according to the following rule:

$$I_F^{(n+1)}(\mathbf{r}) = \left[1-\Delta^{(n)}(\mathbf{r})\right]I_F^{(n)}(\mathbf{r}) + \Delta^{(n)}(\mathbf{r})I_n(\mathbf{r}), \tag{2}$$

where $\Delta^{(n)}(\mathbf{r})$ is referred to as the anisotropic gain and controls locally the weight associated with the fusion of image $I_n(\mathbf{r})$ into the fused image $I_F^{(n)}$. The definition of the anisotropic gain has been modified compared to previous implementations of the LRF algorithm and is now given by

$$\Delta(\mathbf{r}) = \begin{matrix} 0 & \text{for } \frac{M(\mathbf{r})}{M_F(\mathbf{r})} \le \alpha, \\ \frac{M(\mathbf{r})-\alpha M_F(\mathbf{r})}{(\beta-\alpha)M_F(\mathbf{r})} & \text{for } \alpha < \frac{M(\mathbf{r})}{M_F(\mathbf{r})} \le \beta, \\ 1 & \text{for } \frac{M(\mathbf{r})}{M_F(\mathbf{r})} > \beta, \end{matrix} \tag{3}$$

where $M(\mathbf{r})$ and $M_F(\mathbf{r})$ denote the IQM's corresponding to images $I(\mathbf{r})$ and $I_F(\mathbf{r})$ respectively and parameters α and β are chosen so that $1 < \alpha < \beta$. Note in Eq. (3) that the weight map $\Delta(\mathbf{r})$ is directly related to the local image quality improvement with respect to the current fused image as characterized by the ratio $M(\mathbf{r})/M_F(\mathbf{r})$. This ensures the fused image $I_F(\mathbf{r})$ incorporates regions with the best image quality within the set of source images. The parameter α controls the image quality improvement yielded by a new source image $I_n(\mathbf{r})$ required to trigger fusion of a new region. In other words, a source image region needs to have its IQM α-times larger than the IQM of the current fused image in order to be (partially or fully) incorporated. Parameter α is generally set to values slightly above 1 in order to avoid unnecessary fusion of image regions that do not improve significantly the quality of the resulting fused image. Parameter β controls the image quality improvement provided by a new frame required for substituting completely a region [$\Delta(\mathbf{r}) = 1$ in this area] with the new source data.

2.3 Automation of the LRF algorithm

Fusion results obtained using Eq. (2) are characterized by their dependence on the fusion parameter a which controls the size of the lucky-regions being selected and fused [see Eq. (1)]. Choosing a large lucky-region size a causes the algorithm to incorporate more image information from the set of source images into the fused image, at the risk of including areas with low image quality ("inclusive" fusion) and resulting in poor image quality improvements. On the other hand, selecting small lucky-regions provides a better optimization of the local image quality ("selective" fusion) but can result in the apparition of image artifacts[5]. Such artifacts typically consist in edges in the fused image that do not correspond to object features in the scene of interest and that are not induced by the random media distortions ("artificial" edges). These are caused by selecting lucky-regions with excessively abrupt boundaries. In practice, attempts to use a fixed value for the kernel size usually fail when subject to temporal fluctuations of the imaging medium (e.g. variations of the strength of atmospheric turbulence). We introduce a technique for adaptive selection of the fusion kernel that is based on the image content and do not require user intervention.

The LRF technique aims to fuse image regions that are characterized by a high spatial frequency content compared to other areas. For this reason the strategy used to select lucky-regions is based on the analysis of the edge content of the source images: for image sets with high frequency content lucky-regions should be picked in a selective manner (i.e. using a small kernel size a) and vice versa. Automation of the LRF technique consists in (1) computing an edge metric Γ which characterizes the edge content of the image set $\{I_n(\mathbf{r})\}$, and (2) calculating the automated fusion kernel size a_{auto} from metric Γ using an experimental model. The model is established in order to comply with the selective/inclusive fusion tradeoff described previously and is given by

$$a_{auto} = K/\Gamma, \tag{4}$$

where K is a calibration factor. Details about the computation of the Γ can be found in Ref. 5.

3. MULTI-SPECTRAL LRF

The implementation of the LRF algorithm presented in the previous section operates in an automated manner based solely on the content of the set of source images: the fusion kernel diameter a is selected using an edge metric which characterizes the overall sharpness of the set of images to fuse. Processing of multi-spectral data (e.g. visible RGB and IR) using the LRF technique can hence be achieved by repeating the same process for each of the channels and yield distinct values of parameter a. For example, for a set of RGB color images with intensity distributions denoted $\{R_n(\mathbf{r}), G_n(\mathbf{r}), B_n(\mathbf{r})\}$ multi-spectral LRF is performed as follows:

1. The fusion kernel diameter is determined separately for each channel of the color set $\{R_n(\mathbf{r}), G_n(\mathbf{r}), B_n(\mathbf{r})\}$ resulting in diameters given by set $\{a_R, a_G, a_B\}$.
2. Lucky-region fusion is performed on image sets $\{R_n(\mathbf{r})\}$, $\{G_n(\mathbf{r})\}$ and $\{B_n(\mathbf{r})\}$ for the kernel parameter values a_R, a_G and a_B respectively, and result in the fused images $R_F(\mathbf{r})$, $G_F(\mathbf{r})$ and $B_F(\mathbf{r})$.
3. The fused images are combined into a color fused set $\{R_F(\mathbf{r}), G_F(\mathbf{r}), B_F(\mathbf{r})\}$.

Figure 1 illustrates fusion of a sequence of RGB images and Table 1 presents the fusion kernel diameters a_R, a_G and a_B that were obtained from image set content analysis as well as the image quality metric values obtained for each channel prior and after fusion.

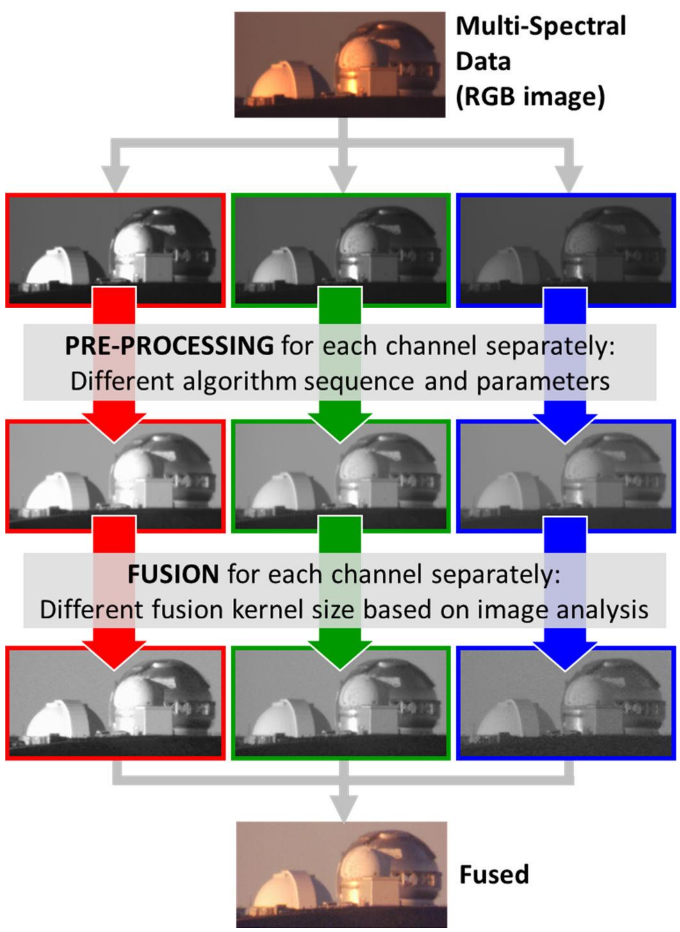

Fig. 1. Illustration of the LRF algorithm applied to a RGB sequence of atmospherically-distorted images. The data set consists of 150 frames captured for an integration period of 4 ms at sunset, using a telescope with an aperture diameter of

210 mm and a focal distance of 2100 mm. The scene being imaged (alt.: 4100 m) was located at a distance of 33 km from the imaging system (alt.: 3400 m).

Table. 1. Image quality metric values corresponding to images in Fig. 1 obtained prior and after pre-processing and lucky-region fusion for each RGB channel and for the resulting fused color image.

	J_R	J_G	J_B	J
Source	1	1	1	1
Pre-processed	1.01	1.19	1.44	1.21
Fused (fusion kernel size)	1.24 (a_R =4.2pix.)	1.49 (a_G =5.5pix.)	2.20 (a_B =8.1pix.)	1.64

Note in Table 1 how the fusion kernel values significantly vary as a result of the different spatial frequency content of each channel. This also leads to various degrees of image quality improvements.

4. HIGH-DYNAMIC RANGE IMAGING

4.1 Introduction

The real world features scenes with light intensities characterized by dynamic ranges orders of magnitude higher than what conventional imaging systems can record. Typically, high dynamic range (HDR) imaging is accomplished in a two-step process. First, a HDR radiance map of a wide range scene is recovered from a set of differently-exposed conventional images [low dynamic range (LDR) images]. Second the HDR map is compressed using tone mapping techniques in order to allow rendering on standard display devices. Such techniques are usually developed for applications for which color and tone reproduction are critical such as computer vision, computer graphics and digital photography. Applications such as medical imaging and surveillance favor detail visualization at the expense of a natural appearance of the scene and HDR imaging can directly be achieved by fusing LDR images with no need to tone mapping.

4.2 HDR lucky-region fusion

We propose to use the LRF technique for simultaneously improving the rendering of high dynamic range scenes and mitigating random local distortions such as the ones introduced by atmospheric turbulence. HDR lucky-region fusion is performed according to the following steps:

- **Step 1:** N_T sets of images of the same scene are captured each for a different integration (exposure) period T_i, $i \in [1, N_T]$. Each of the recorded sets, denoted $\{I_n^{T_1}(\mathbf{r})\}$, $\{I_n^{T_2}(\mathbf{r})\}$,..., $\{I_n^{T_{N_T}}(\mathbf{r})\}$, hence encompasses a different portion of the scene's dynamic range.

- **Step 2:** The LRF algorithm described in section 2 is applied to each set $\{I_n^{T_1}(\mathbf{r})\}$, $\{I_n^{T_2}(\mathbf{r})\}$,..., $\{I_n^{T_{N_T}}(\mathbf{r})\}$ resulting in N_T fused images $I_F^{T_1}(\mathbf{r})$, $I_F^{T_2}(\mathbf{r})$, ..., $I_F^{T_{N_T}}(\mathbf{r})$ for which the degrading effect of atmospheric turbulence is mitigated. These fused images constitute a set $\{I_F^{T_i}(\mathbf{r})\}$ of low-dynamic range images each characterized by integration time T_i.

- **Step 3:** The LRF algorithm is now applied to the set of LDR images $\{I_F^{T_i}(\mathbf{r})\}$ yielding a fused image $I_F(\mathbf{r})$ that (1) provides an improved visualization of a HDR scene, and (2) features a mitigated effect of random local distortions.

Lucky-region fusion applied to atmospherically-distorted images (step 2) and LRF applied to differently-exposed images (step 3) can be performed in a reversed order (step 3 then step 2) or in an interleaved manner (step 2, step 3, step 2, etc.). These different fusion strategies still require further investigation.

Figure 2 presents experimental results for $N_T = 2$ sets of images captured with exposure periods $T_1 = 3.1$ ms and $T_2 = 8$ ms. The atmospherically-distorted LDR sets are denoted $\{I_n^{T_1}(\mathbf{r})\}$ and $\left\{I_n^{T_2}(\mathbf{r})\right\}$ and each composed of $N = 100$ frames. Images resulting from the fusion of sets $\{I_n^{T_1}(\mathbf{r})\}$ and $\{I_n^{T_2}(\mathbf{r})\}$ -- denoted $I_F^{T_1}(\mathbf{r})$ and $I_F^{T_2}(\mathbf{r})$ -- are shown in Fig. 2(a) and 2(b) respectively. Note how in Fig. 2(b) some regions of the image are over-exposed and the corresponding image is saturated (white areas) as result of the limited dynamical range of the photo-sensor. The lucky-region fusion algorithm will exclude these areas since computation of the image quality map $\Delta(\mathbf{r})$ will produce near-zero values (no sharp edges present). Similarly, under-exposed image regions will be excluded by the LRF process. On the other hand image regions under-exposed in image 2(a) appear more clearly in 2(b) as the exposure period increases (see red arrows). Fusion of images $I_F^{T_1}(\mathbf{r})$ and $I_F^{T_2}(\mathbf{r})$ results in image $I_F(\mathbf{r})$ shown in Fig. 2(c) which includes "properly-exposed" image regions from 2(a) and 2(b).

(a)

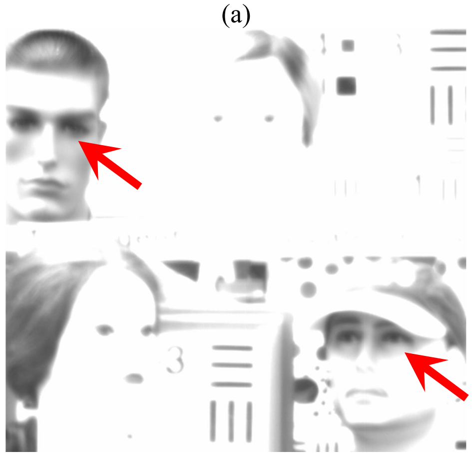

(b)

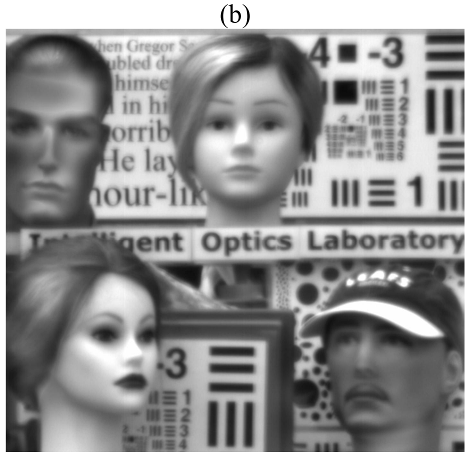

(c)

Fig. 2. Example of HDR lucky-region fusion applied to $N_T = 2$ sets of differently-exposed image sets (T_1 =3.1 ms and T_2 =8 ms) each composed of 100 frames. LRF applied to both set results in images shown in 2(a) and 2(b) respectively. Sub-sequent LRF applied to images in 2(a) and 2(b) results in an image which allows visualization of a broader dynamic range as shown in 2(c). The scene shown is constituted of human-sized mannequin heads and letter-sized target boards imaged at a distance of 250 meters over a near-ground (<3 meters) propagation path.

REFERENCES

[1] Carhart, G. W. and Vorontsov, M. A., "Synthetic imaging: nonadaptive anisoplanatic image correction in atmospheric turbulence," Opt. Let., 23, 745-747 (1998).

[2] Vorontsov, M. A., "Parallel image processing based on an evolution equation with anisotropic gain: integrated optoelectronic architectures," J. Opt. Soc. Am. A, 6, 1623-1637 (1999).

[3] Vorontsov, M. A. and Carhart, G. W., "Anisoplanatic imaging through turbulent media: image recovery by local information fusion from a set of short-exposure images," J. Opt. Soc. Am. A, 18, 1312-1324 (2001).

[4] Aubailly, M., Vorontsov, M. A., Carhart, G. W. and Valley, M. T., "Image enhancement by local information fusion with pre-processing and composed metric," Atmospheric Optics: Models, Measurements, and Target-in-the-Loop Propagation II, Proc. of SPIE, 7090 (2008).

[5] Aubailly, M., Vorontsov, M. A., Carhart, G. W. and Valley, M. T., "Automated video enhancement from a stream of atmospherically-distorted images: the lucky-region fusion approach," Atmospheric Optics: Models, Measurements, and Target-in-the-Loop Propagation III, Proc. of SPIE, 7463 (2009).